Fine Sediments Dynamics in the Marine Environment Proceedings of INTERCOH-2000.
ed. J.C. Winterwerp and C. Kranenburg, **Elsevier, p. 595-610.**

3-D numerical modelling of mud and radionuclide transport in the Chernobyl Cooling Pond and Dnieper - Boog Estuary

N. Margvelashvili, V. Maderich, S.Yuschenko and M. Zheleznyak

Institute of Mathematical Machine and System Problems,
Glushkova av. 42, Kiev, 03187, The Ukraine.

The 3-D model THREETOX, that includes modules of hydrodynamics, sediment and pollutant transport, was developed to simulate the radionuclide fate in a deep stratified water body. This paper describes the methodology and results of simulation of the radionuclide transport and fate in the cooling pond of the Chernobyl Nuclear Power Plant and in the Dnieper – Boog Estuary. The analysis of the efficiency of the chosen sediment transport model is based on the use of radionuclides from the Chernobyl accident as tracer.

Modelling; sediment transport; mud; radionuclide transport; Chernobyl accident

1. INTRODUCTION

In natural streams affected by human pollution – heavy metals, radionuclides, PCB, nutrients and others - suspended sediments play a role as the carriers of contaminants over long distances from the release areas. The processes of sedimentation and erosion of contaminated sediments drive the re-distribution of the pollutant in the bed sediment. The magnitude of the partition coefficient that describes the distribution of contaminant between the liquid and solid phases increases usually with decreasing sediment grain size. Therefore, models describing the transport and fate of suspended sediments are the important parts of the modelling system for the simulation of pollutant transport in water bodies (Onishi et al., 1981; Santschi et al., 1989; Perianez, 2000). However, immediate data on cohesive sediment transport are rarely available for many natural water bodies. In this respect radioactive isotopes, treated as tracers, could provide an efficient tool for studying the mud behaviour in surface waters.

After the Chernobyl accident, a set of models was developed to simulate the fate and behavior of the Chernobyl radionuclides in water bodies in the vicinity of the Chernobyl Nuclear Power Plant (NPP) and in the Dnieper river/reservoir system (Zheleznyak et al., 1992;1997). The recently developed 3-D model THREETOX, that includes modules for hydrodynamics, sediment transport and pollutant transport, has been applied to deep stratified water bodies contaminated after the Chernobyl accident (Margvelashvili et al., 1997; Koziy et al., 1998; Margvelashvili et al., 1999).

The aim of this paper is the extension of the THREETOX model for the simultaneous description of different sediment fractions, including cohesive sediments. The model is applied to study the fate and behavior of radionuclides in the highly contaminated Cooling Pond of the NPP and in the Dnieper-Boog Estuary. The analysis of the efficiency of the

chosen sediment transport model is based on the use of the radionuclides released during the Chernobyl accident as tracer.

2. MODEL

2.1. Hydrodynamics

The hydrodynamics of THREETOX model are based on the three-dimensional, time-dependent, free surface model of Blumberg and Mellor (1987). The prognostic variables of the hydrodynamics code are the three components of velocity, the temperature, salinity and surface elevation fields. The governing equations are:

$$\vec{\nabla}\cdot\vec{U}=0, \tag{1}$$

$$\frac{\partial U}{\partial t}+\vec{U}\cdot\vec{\nabla}U-fV=-\frac{1}{\rho_0}\frac{\partial P}{\partial x}+\frac{\partial}{\partial z}\left(\nu\frac{\partial U}{\partial z}\right)+A\Delta U, \tag{2}$$

$$\frac{\partial V}{\partial t}+\vec{U}\cdot\vec{\nabla}V+fU=-\frac{1}{\rho_0}\frac{\partial P}{\partial y}+\frac{\partial}{\partial z}\left(\nu\frac{\partial V}{\partial z}\right)+A\Delta V, \tag{3}$$

$$\frac{\partial (T,S)}{\partial t}+\vec{U}\cdot\vec{\nabla}(T,S)=\frac{\partial}{\partial z}\left(\nu_T\frac{\partial (T,S)}{\partial z}\right)+A_T\Delta(T,S), \tag{4}$$

$$\rho=\rho(T,S), \tag{5}$$

$$P(x,y,z,t)=P_0+g\rho_0(\eta-z)+g\int_z^{\eta}\rho(x,y,z',t)dz' \tag{7}$$

The concept of eddy viscosity (ν), diffusivity (ν_T) and the Prandtl hypothesis, with variable turbulence length scale, are used to define the turbulence stresses and fluxes. The vertical turbulent exchange coefficients are:

$$\begin{cases} \nu_T=k_1^2z^2\left(1-\dfrac{z}{H}\right)^2\left|\dfrac{\partial\vec{U}}{\partial z}\right|\left(1-\dfrac{Ri}{Ri_c}\right)^{1/2}, & 0<Ri<Ri_c \\ \nu_T=0.0, & Ri\geq Ri_c \\ \nu=\nu_T(1+Ri) \end{cases} \tag{8}$$

Here $\vec{U}=(U,V,W)$ is the velocity vector, T is the temperature, S is the salinity, η is the free surface elevation, f is the Coriolis parameter, P is the pressure, ρ and ρ_o are the calculated and the standard density of water, g is the acceleration due to gravity, A and A_T are the coefficients of turbulent horizontal viscosity and the temperature diffusivity, respectively, and $Ri=-\dfrac{g(\partial\rho/\partial z)}{\rho_0\left(\partial\vec{U}/\partial z\right)^2}$ is the Richardson number, $k_1=0.1$, $Ri_c=10$.

At the free surface all fluxes (momentum, heat, etc.) are prescribed. At the bottom and at the land boundaries, the conditions of zero diffusive fluxes of all properties are used. The open lateral boundary conditions are modified radiation conditions.

2.2. Sediment transport

All particulate matter is represented by three different grain size fractions. The effect of sediment on the hydrodynamics is neglected. Suspended sediment transport is described by the advection- diffusion equation, taking into account the settling velocity of the sediment:

$$\frac{\partial S_{di}{}^{w}}{\partial t}+U\frac{\partial S_{di}{}^{w}}{\partial x}+V\frac{\partial S_{di}{}^{w}}{\partial y}+(W-W_{gi})\frac{\partial S_{di}{}^{w}}{\partial z}=\frac{\partial}{\partial z}\left(\nu_T\frac{\partial S_{di}{}^{w}}{\partial z}\right)+A(\Delta S_{di}{}^{w}), \tag{9}$$

where $S_{di}{}^{w}$ is the concentration of i-th fraction of sediment in the water column, and W_{gi} is settling velocity of solid particles. At the free surface, zero vertical sediment flux is assumed, i.e:

$$(W-W_{gi})S_{di}{}^{w}=\nu_T\frac{\partial S_{di}{}^{w}}{\partial z},\ \mathrm{z}=\eta. \tag{10}$$

The vertical flux of suspended sediments at the bottom is equal to the difference between the resuspension and sedimentation rate:

$$\nu_T\frac{\partial S_{di}{}^{w}}{\partial z}+W_{gi}S_{di}{}^{w}=q_i{}^{w}-q_i{}^{b},\qquad z=-h+z_0, \tag{11}$$

where h is the depth, z_0 is the bottom roughness, $q_i{}^{w}$, $q_i{}^{b}$ are the sedimentation and resuspension rates, respectively. The concentration of sediments in the upper bottom layer is described by the following equation:

$$\frac{\partial(m_{di}{}^{b})}{\partial t}=q_i{}^{w}-q_i{}^{b}, \tag{12}$$

where $m_{di}{}^{b}=S_{di}{}^{b}Z_*$ is the mass of i-th fraction of bottom sediment per unit area, and Z_* is the depth within the bottom sediment top layer. The thickness of the bottom layer and bed porosity are defined from the relationships:

$$\tilde{Z}=\frac{1}{1-\varepsilon}\sum_{i\ solid}\frac{m_{di}{}^{b}}{\rho_{Si}},\qquad \tilde{\varepsilon}=\frac{V_{tot}-\sum\limits_{i\ solid}V_i}{V_{tot}}=\frac{Z_{\min}-\sum\limits_{i\ solid}\dfrac{m_{di}{}^{b}}{\rho_{Si}}}{Z_{\min}}, \tag{13}$$

$$Z_*=\begin{cases}\tilde{Z},\ \varepsilon=\varepsilon_0=const,\ \tilde{Z}>Z_{\min}\\ \\ Z_{\min},\ \varepsilon=\tilde{\varepsilon},\ \tilde{Z}\le Z_{\min}\end{cases}, \tag{14}$$

where ε is the porosity of the bed layer, V_i is the volume of i-th fraction of the sediments, ρ_{Si} is the density of the solid particles. From eqns. (12) and (14) the concentration of the i-th fraction of sediment in the bottom layer is defined as:

$$S_{di}{}^{b}=\frac{m_{di}{}^{b}}{Z_*}. \tag{15}$$

For cohesive sediment the erosion and deposition rates are modelled by using the formulae of Ariathurai and Krone (1976). For non-cohesive sediments the bottom boundary condition describes the resuspension or settling of sediments, which depends on the ratio between the actual and the near-bed equilibrium concentration of the sediments. The latter one is estimated

according to Van Rijn (1984). The effective bottom shear stresses induced by currents and wind waves are summed. The formula derived on the basis of numerical solution of the equations for oscillating bottom boundary layer (Zheleznyak, 1988) was used to parameterise the wave induced stresses.

2.3. Radionuclide transport

The sub-model of radionuclide transport describes the specific water-sediment sorption processes. It includes the advection-diffusion equations for dissolved ($C_s^{\,w}$) and adsorbed by suspended sediment ($C_p^{\,w}$) radioactivity in the water column, and the equations for concentration of the dissolved ($C_s^{\,b}$) and adsorbed ($C_p^{\,b}$) radioactivity in the bottom deposits:

$$\frac{\partial C_s^{\,w}}{\partial t}+\frac{\partial UC_s^{\,w}}{\partial x}+\frac{\partial VC_s^{\,w}}{\partial y}+\frac{\partial WC_s^{\,w}}{\partial z}= \frac{\partial}{\partial z}\left(\nu_T\frac{\partial C_s^{\,w}}{\partial z}\right)+A(\Delta C_s^{\,w})-\lambda C_s^{\,w}-a_{1,2}^{\,w}(S_d^{\,w}K_d^{\,w}C_s^{\,w}-C_p^{\,w}), \tag{16}$$

$$\frac{\partial C_p^{\,w}}{\partial t}+\frac{\partial UC_p^{\,w}}{\partial x}+\frac{\partial VC_p^{\,w}}{\partial y}+\frac{\partial (W-W_g)C_p^{\,w}}{\partial z}= \frac{\partial}{\partial z}\left(\nu_T\frac{\partial C_p^{\,w}}{\partial z}\right)+A(\Delta C_p^{\,w})-\lambda C_p^{\,w}+a_{1,2}^{\,w}(S_d^{\,w}K_d^{\,w}C_s^{\,w}-C_p^{\,w}), \tag{17}$$

$$\frac{\partial m_s^{\,b}}{\partial t}=\frac{F_{dif}}{Z_*}(C_s^{\,w}-\frac{C_s^{\,b}}{\varepsilon})-a_{1,2}^{\,b}(\frac{S_d^{\,b}}{\varepsilon}K_d^{\,b}C_s^{\,b}-C_p^{\,b})\cdot Z_*-\lambda m_s^{\,b}, \tag{18}$$

$$\frac{\partial m_p^{\,b}}{\partial t}=(\frac{C_p^{\,w}\sum\limits_{i\,solid}q_i^{\,w}}{\sum\limits_{i\,solid}S_{di}^{\,w}}-\frac{C_p^{\,b}\sum\limits_{i\,solid}q_i^{\,b}}{\sum\limits_{i\,solid}S_{di}^{\,b}})+a_{1,2}^{\,b}(\frac{S_d^{\,b}}{\varepsilon}K_d^{\,b}C_s^{\,b}-C_p^{\,b})\cdot Z_*-\lambda m_p^{\,b}, \tag{19}$$

where $m_s^{\,b}=C_s^{\,b}Z_*$, $m_p^{\,b}=C_p^{\,b}Z_*$, $S_d^{\,w}=\sum\limits_{i\,solid}S_{di}^{\,w}$, $C_p^{\,w}=\sum\limits_{i\,solid}C_{pi}^{\,w}$, $W_g=\sum\limits_{i\,solid}W_{gi}S_{di}^{\,w}/S_d^{\,w}$, $S_d^{\,b}=\sum\limits_{i\,solid}S_{di}^{\,b}$, $C_p^{\,b}=\sum\limits_{i\,solid}C_{pi}^{\,b}$, λ is the radionuclide decay constant, and F_{dif} is the diffusion coefficient. The governing equations of the model are similar to those used in the FLESQOT model (Onishi et al., 1989).

The exchanges between the different phases are described by diffusion, sorption, and sedimentation-resuspension processes. Adsorption and desorption of radionuclides between liquid and solid phases are described by the radionuclide exchange rates $a_{1,2}^{\,w}$ $a_{1,2}^{\,b}$, and by the distribution coefficients $K_d^{\,w}, K_d^{\,b}$ (Onishi et al., 1981; Santschi and Honeyman, 1989;

IAEA, 1985; Carrol and Harms 1999), which are defined, under steady hydraulic conditions, as

$$S_d{}^w K_d{}^w = \lim_{t\to\infty}\left(\frac{C_p{}^w}{C_s{}^w}\right), \qquad \frac{S_d{}^b}{\varepsilon} K_d{}^b = \lim_{t\to\infty}\left(\frac{C_p{}^b}{C_s{}^b}\right). \tag{19}$$

At the free surface $z = \eta$ the boundary conditions are:

$$v_T \frac{\partial C_s{}^w}{\partial z} = W C_s{}^w, \quad (W - W_g) C_p{}^w - v_T \frac{\partial C_p{}^w}{\partial z} = 0, \tag{20}$$

The fluxes into the bottom $z = -h + z_0$ are:

$$v_T \frac{\partial C_s{}^w}{\partial z} = \frac{F_{dif}}{Z_*}\left(C_s{}^w - \frac{C_s{}^b}{\varepsilon}\right), \tag{21}$$

$$v_T \frac{\partial C_p{}^w}{\partial z} + (W - W_g) C_p{}^w = \frac{C_p{}^w \sum_{i\ solid} q_i{}^w}{\sum_{i\ solid} S_{di}{}^w} - \frac{C_p{}^b \sum_{i\ solid} q_i{}^b}{\sum_{i\ solid} S_{di}{}^b}, \tag{22}$$

In THREETOX, σ-coordinate transformation is applied to avoid difficulties in the numerical solution for realistic bottom topography. Splitting of the barotropic and baroclinic modes are imposed in the code. The governing equations together with the boundary conditions are solved by finite difference techniques. A horizontally and vertically staggered mesh is used for the computations.

3. CASE STUDIES

3.1. Chernobyl NPP cooling pond

The Chernobyl Cooling Pond (ChCP) was constructed in 1972 in the floodplain of the River Pripyat. The length is 11.5 km, the maximum width is 2.2 km, the maximum depth is 18 m, and the volume is 0.16 km^3 (Figure 1). The water level in the ChCP, 6 m above the River Pripyat level, is kept constant by pumping of the river water into the cooling pond to compensate the losses due to seepage and evaporation. Currents in the ChCP were driven by the discharge and intake of cooling water, and by wind and baroclinic effects. During the operation of the NPP, the water mass of the ChCP had significant temperature stratification with temperature gradients up to 10°-12°C. The upper layer of the bed consists mainly of mud. The ChCP was heavily contaminated by the Chernobyl accident in April-May, 1986. Till today, the concentrations of ^{137}Cs and ^{90}Sr in the bottom sediments are rather high. Field measurements revealed redistribution and accumulation of the radionuclide in deepest parts of the cooling pond. At present, the model studies on the fate and behaviour of radionuclide in the ChCP are stimulated by the needs to assess the radionuclide re-distribution after the closure of the Chernobyl NPP in December, 2000.

The dynamics of ^{137}Cs in the ChCP over one year after the accident has been simulated. The regime of the water discharge used in the simulations as boundary condition, is shown in Table 1. The temperature of cooling water entering the Cooling Pond was set 10^o C above the temperature in the water intake channel. Ten days averages of the temperature of the atmosphere, and of wind characteristics were used to specify the boundary conditions at the surface.

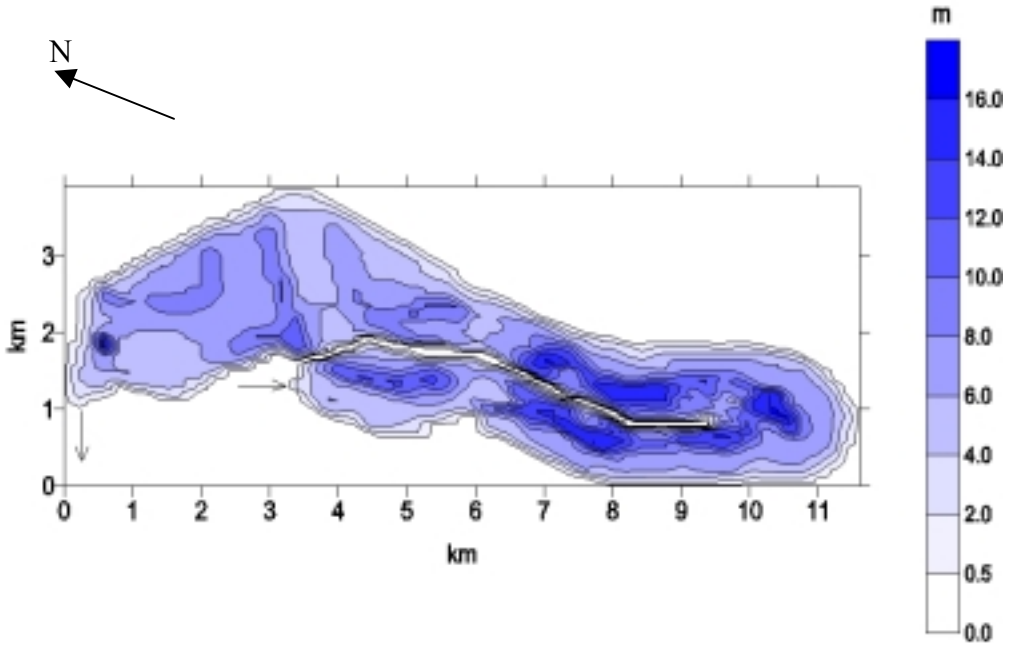

Figure 1. Depth distribution in the ChCP. The arrows show the cooling water intake and outfall.

The atmospheric fallout of the radionuclide at the surface of the pond was modelled by instantaneous, non-homogeneous deposition (Figure 2) based on the interpolation of the density of the ^{137}Cs deposition on the soil around the ChCP (Shiklomanov, 1992). Sediment and radionuclide fluxes in the water discharge channel were set equal to those in the water intake channel. The parameter values were $K_d{}^b$=3 m^3/kg, $a_{1,2}{}^w = 1\,\mathrm{d}^{-1}$ and $a_{1,2}{}^b = 1\,\mathrm{y}^{-1}$. To estimate the sensitivity of the computational results to variations in the distribution coefficient, the calculations were carried out for $K_d{}^w$ = 3 m^3/kg and for $K_d{}^w$=15 m^3/kg as well.

Simulations have been carried out for three suspended sediment diameters: 5, 15 and 30 μm, and an aerosol sediment flux at the water surface $5\cdot10^{-6}$ kg m^{-2}s^{-1}. The resolution of the numerical grid in the horizontal directions was 500 × 150 m. Vertical coordinate was resolved by 11 equally-spaced levels. The spatial distribution of the different fractions of the bottom sediments of the pond measured in 1983 (Shiklomanov, 1992) shows an intensive accumulation of the clay sediments in the deepest parts of the pond (Figure 3).

Table 1.
Water flow through the discharge channel in 1986.

Date	1-26 April	27 Apr.-30 Sept.	1 -31Oct	1 –30 Nov	1 - 31 Dec.
Discharge (м^3/s)	200	15	50	100	150

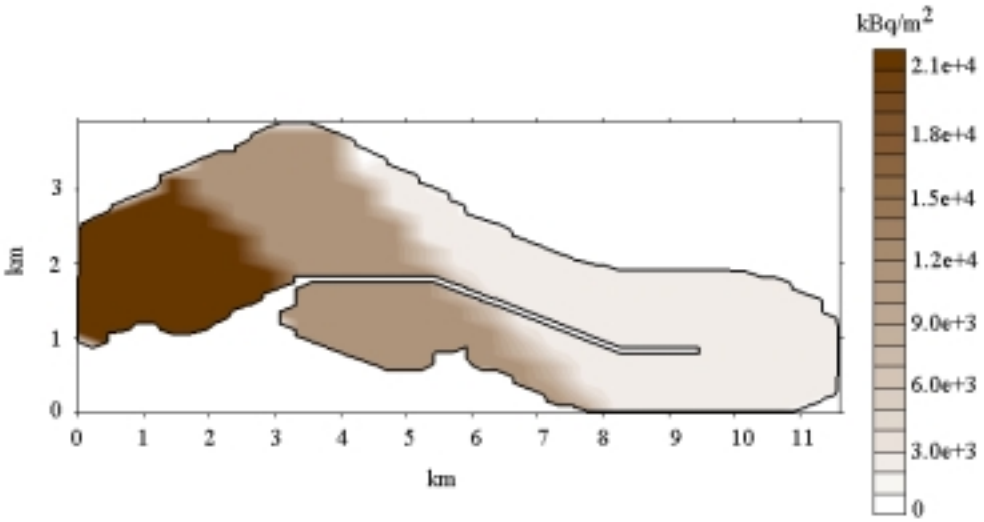

Figure 2. Estimated fallout of ^{137}Cs at the surface of ChCP in April 1986.

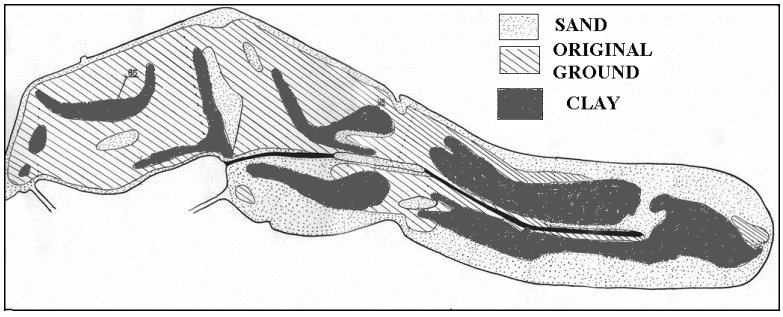

Figure 3. Observed distribution of bottom sediments in ChCP in 1983 (Shiklomanov, 1992).

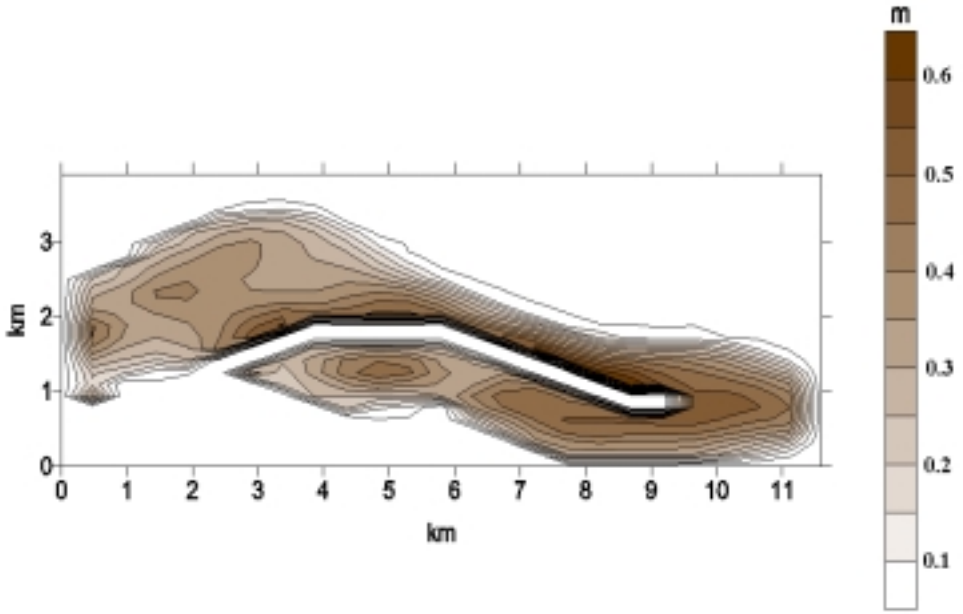

Figure 4. The simulated deposition rate integrated over 10 years period.

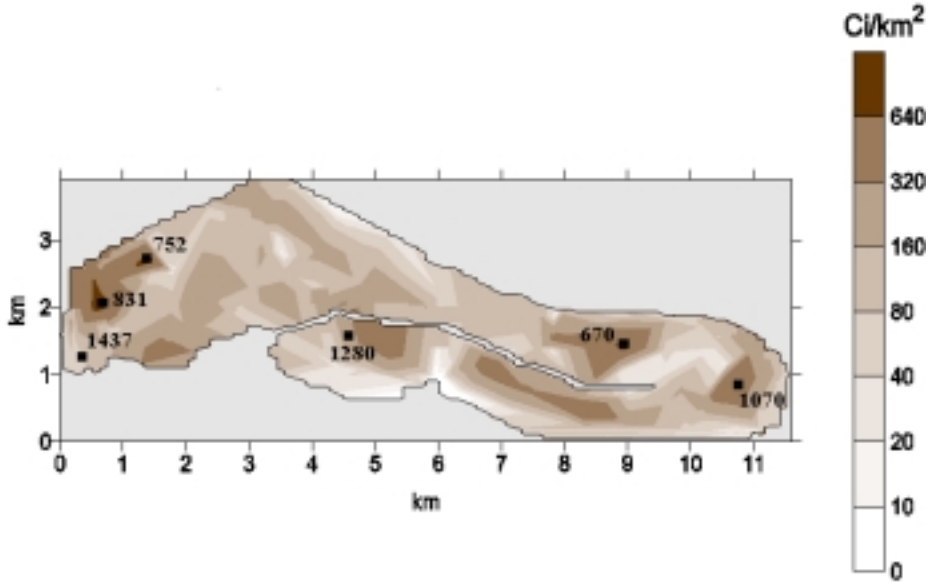

(a)

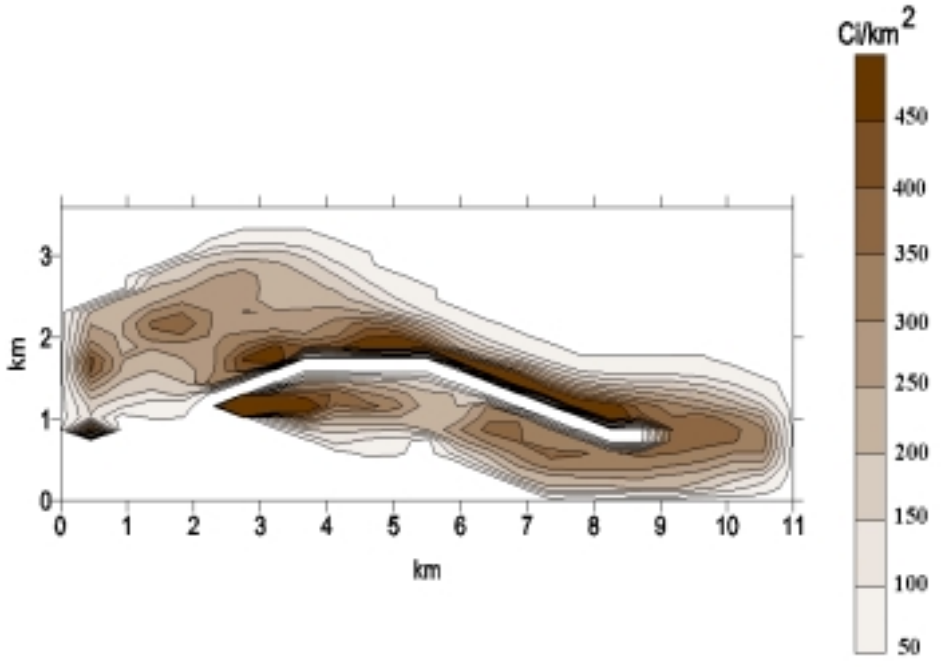

(b)

Figure 5. Measured (Shiklomanov, 1992) (a) and computed (b) distributions of ^{137}Cs in the bottom sediments of ChCP.

The deposition rate was simulated by THREETOX for one year and then linearly extrapolated for a period of 10 year. The computed spatial distribution deposition in the pond (Figure 4) is similar to the measurements (Figure 3). The distributions of ^{137}Cs in the bottom sediments as measured in 1989 (Shiklomanov, 1992) and simulated over one year (from 1986 to 1987) are shown in Figure 5. Both computed and measured distributions of the bottom contamination correlate with the pattern of the sedimentation rate in the ChCP as shown in Figure 3.

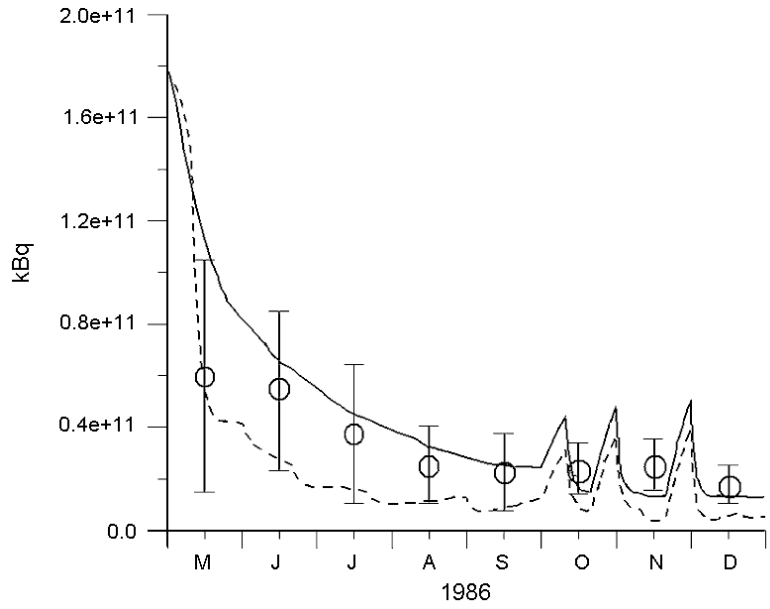

Figure 6. Computed and measured contents of the ^{137}Cs in the water column of CPP. The solid line corresponds to K_d^w = 3 m^3/kg, the dashed line corresponds to K_d^w=15 m^3/kg.

Measured (Shiklomanov, 1992) and computed ^{137}Cs contents in the water column of the pond are depicted in Figure 6. Peaks on the curves in the autumn and winter are explained by the storm events resulting in resuspension of contaminated bottom sediments. According to the simulations, more than 95 % of total ^{137}Cs in the cooling pond had been deposited into the bottom sediments before the end of 1986. This is in agreement with the estimate BIOMOVS (1996).

3.2. Dnieper-Boog estuary

The Dnieper-Boog Estuary (DBE), located on the north-west coast of the Black Sea, is the largest estuary of this sea, with a surface area of 1006.3 km^2 and a volume of 4.24 km^3 (Figure 7). It is connected with the Black Sea through the Kinbourn Strait, located at the left-hand side of the figure. The regime of this drowned-river estuary varies from stratified to partially mixed. The sources of freshwater discharge are the River Dnieper and the River Southern Boog. DBE is at the end of Chernobyl's riverine radionuclide transport from the Chernobyl accident area to the Black Sea. The bottom sediments in the DBE are sandy at the river mouths. The bottom sediments in the other parts of the DBE mainly consist of cohesive sediments.

The simulation of the dispersion of radionuclides that entered the DBE after the Chernobyl accident was carried out for the period May 1986 - April 1988. To diminish the effect of the uncertainty sea level variations at the open boundary, the calculations were carried out in two nested areas. Temperature, salinity, velocity and sea elevation fields of the North -Western Black Sea resulting from a large area model calculation, were used as open boundary conditions for a nested model of higher resolution. The monthly-averaged wind, with a stochastic component, and the monthly-averaged air temperature were specified according to Simonov and Altman (1991).

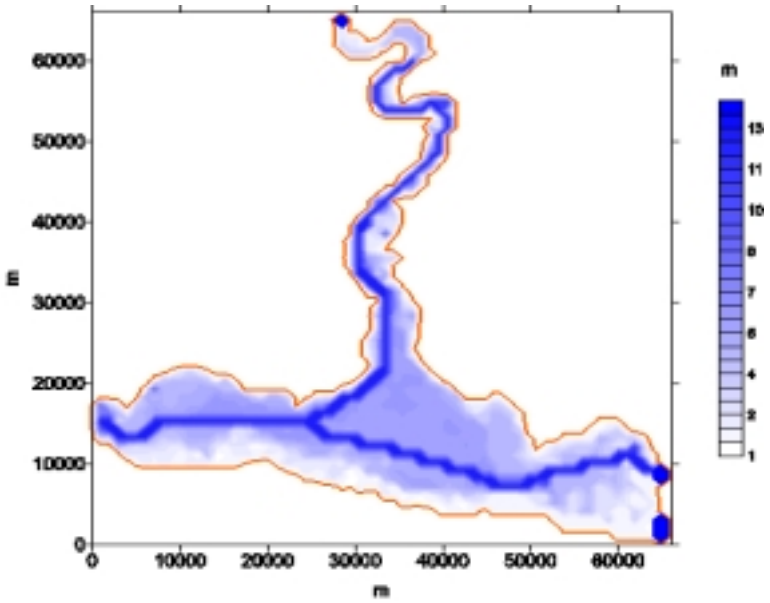

Figure 7. The bathymetry of the DBE.

The monthly-averaged concentrations of suspended sediment at the mouth of the River Dnieper and at the mouth of the River Southern Boog were specified according to data from the State Water Cadastre. The initial thickness of the upper bottom sediment layer was set at 2 cm. Monthly-averaged concentrations of dissolved and adsorbed radionuclides in the river water at the mouths of the Dnieper and the Southern Boog were prescribed by using data from Batrakov et al. (1994), Polikarpov et al. (1988) and Polikarpov et al. (1992).

The computed salinity, presented in Figure 8, is compared with survey data that are represented in the figure by the values with decimals. The salt-water intrusion into the DBE takes place mainly in the summer season, when the water discharge from the River Dnieper is low. Along the navigational channel of the DBE, the density-induced deep undercurrent results in a wedge of salty Black Sea water.

In Figure 9, the computed vertical distributions of dissolved ^{137}Cs and ^{90}Sr along the DBE and adjacent shelf are shown for July 1987. The patterns of isolines for the ^{137}Cs and ^{90}Sr concentrations are similar, but the concentration gradients are opposite for the two radionuclides. The concentrations of ^{137}Cs increase seawards and towards the bottom, while those of ^{90}Sr decrease. Differences between distribution of dissolved ^{137}Cs and ^{90}Sr concentrations in the mouth of the River Dnieper are explained by the differences in atmospheric fallout and by the behaviour of these radionuclides throughout the River Dnieper basin. As noted by Voitsekhovich (1997) almost 100% of ^{137}Cs, but 70% of ^{90}Sr having reached the River Dnieper, was deposited in the chain of reservoirs of the river.

The correlation of the dissolved radionuclide concentration and the salinity describes the mixing processes in an estuary. Deviations of the salinity (S) and the radionuclide concentration (C) from the area-averaged values ($\overline{S}$ and $\overline{C}$, respectively) were normalised to the maximum difference in salinity, ΔS, and to the radionuclide concentration ΔC in the area, respectively, to produce a non-dimensional representation (Figure 10). The computed data points represent the spring, summer, autumn and winter seasons of 1987. Both ^{137}Cs and ^{90}Sr data points converge into characteristic curves. To clarify the reason for the non-linear character of the dependence between ^{137}Cs and salinity, an additional simulation was carried

out without exchange between the dissolved and attached phases. The calculated points showed a perfect linear correlation, represented by the straight line (2) in Figure 10b. Consequently, the non-linear character of the correlation between the salinity and the dissolved ^{137}Cs concentration in water was due to the exchange of ^{137}Cs with bottom and suspended sediments.

Field data of Polikarpov et al. (1988), collected over the north-western shelf in 1989, are represented by crosses in Figure 10b. They correlate quite well with the computational results. Due to a relatively weak exchange of dissolved ^{90}Sr with sediments, the correlation between salinity and dissolved radionuclide concentration was nearly linear (Figure 10b). The relatively weak quadratic deviations from linearity are due to the non-equilibrium mixing processes in the spring and in the autumn of 1987.

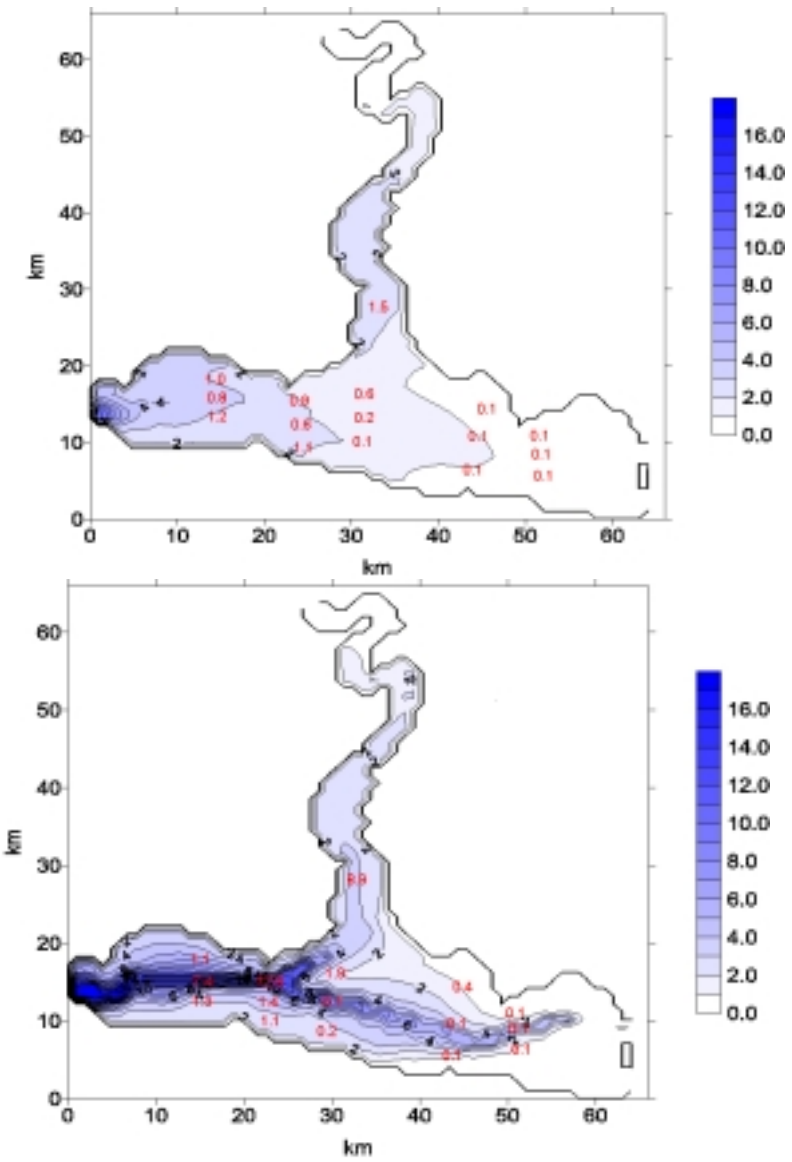

Figure 8. Calculated and observed salinity at the surface and on the bottom of the DBE in June 24, 1987.

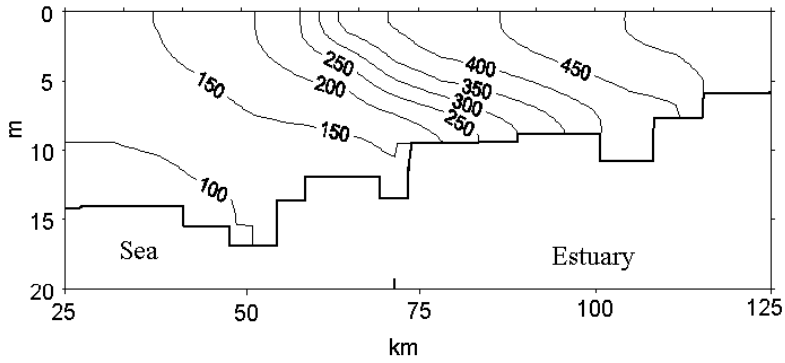

(a)

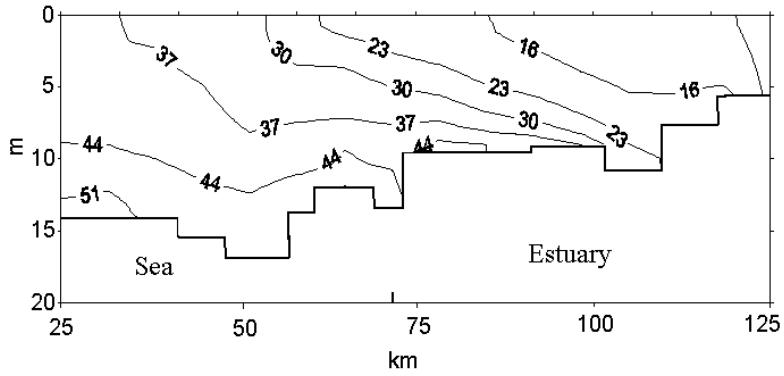

(b)

Figure 9. Computed vertical distribution of dissolved ^{137}Cs (a) and ^{90}Sr (b) along the DBE and north-western shelf in July 1987.

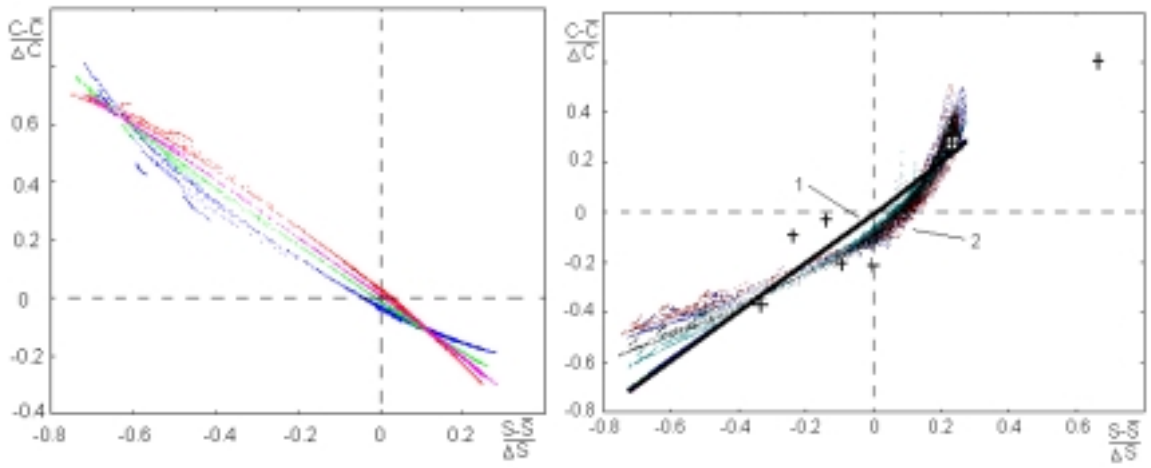

(a) (b)

Figure 10. Correlation between the dissolved ^{90}Sr concentration and salinity (a); Correlation between the dissolved ^{137}Cs concentration and salinity (b).

Calculations showed, that in the spring of 1988 more than 90% of the total ^{137}Cs inventory (0.72 TBq) in the DBE was deposited in the bottom sediments, while 76% of the total ^{90}Sr inventory (1.3 TBq) was in the dissolved phase. The ^{137}Cs flux from the DBE to the Black Sea, during May 1986 till April 1988, was found to be equal to 0.67 TBq, 48 % from the total flow into the DBE (1.39 TBq), while the ^{90}Sr outflow from the DBE to the Black Sea was equal to 15.5 TBq, 92 % from the total inflow (16.8 TBq).

4. DISCUSSION AND CONCLUSIONS

The 3-D simulation of the fate of radionuclides in the Cooling Pond of the Chernobyl NPP in the period 1986-1992 was performed on the basis of initial atmospheric fallout data. There is reasonable agreement between measured and computational data for the radionuclide concentration in the water and in the bottom sediments. Both cohesive sediments and radionuclides were more intensively deposited in deepest parts of the cooling pond. The model reproduced the role of mud sedimentation as a main factor determining the location of the most contaminated spots of bottom sediments of this deep water body.

The Chernobyl NPP has been closed in December 2000 as an installation for nuclear energy production. However, because of technological reasons the cooling pond will be maintained in the current condition for the next several years. After this period, the pumping of river water into the cooling pond will be terminated and its water level will drop to 6 m, leaving 50% of the sediments exposed to the atmosphere. This is considered as a potential source of radiological risk for further wind resuspension. A modelling tool should be developed to predict the ^{137}Cs redistribution in the bed during this period and to support the remediation strategies. The results of the present study show that the proposed approach based on the simulation of dynamics of 3-D fields of suspended sediments and radionuclides in the pond could be used as background for such a tool. The dominant role of mud sedimentation in the redistribution of ^{137}Cs in bottom deposition of the Chernobyl Cooling Pond was confirmed by this study. Therefore, 3-D models that could perform an accurate simulation of mud dynamics should be used to simulate the dynamics of the bed contamination according to the scenarios of the diminishing of the pond's water level and to support the remediation activities.

At the edge of the salt intrusion into an estuary, the radionuclide deposition rate into the bottom increases under the influence of two processes. The first process is flocculation in these areas that intensifies the sedimentation rate. The second process is the increase of the sediment contamination due to higher values of the distribution (partition) coefficient in salt water in comparison with the typical values for fresh water. While some studies were undertaken to show that the distribution coefficients are dependent upon salinity, it is still difficult to define a certain parameterization for this complicated, sorption driven, mechanism (Carrol and Harms, 1999). Therefore during these model runs, a single distribution coefficient value was used for the whole estuary. The ranges of the distribution coefficient values, as used within this study, cover the overlapping ranges of estimates of the fresh and salt water distribution coefficients (Onishi et al. 1981; IAEA, 1985). The undertaken 3-D modeling study shows that differences in the total fluxes and distribution of radionuclide having mid-magnitude (^{137}Cs) and low-magnitude (^{90}Sr) distribution coefficient values could be

quantified on the basis of the chosen schematization of the sediment transport and of the radionuclide – sediment exchange processes.

The model should be improved taking into account the influence of flocculation on 3-D mud transport and using distribution coefficients depending on salinity to simulate the increase of radionuclide scavenging in the mixing zones of fresh and salt water. The collection and processing of data on radionuclide concentration in bottom sediments in estuaries together with hydrological data could lead to the basis for such model refinement.

ACKNOWLEDGEMENTS

We would like to thank Rudie Heling (NRG, The Netherlands) for valuable comments on the manuscript. This article benefited from the comments and suggestions of two anonymous reviewers. The work was partially supported by the EU Contract RODOS, INTAS 97-31278 and by contract of the Ukrainian Ministry of Emergencies and Population Protection Affairs from Consequences of the Chernobyl Catastrophe.

REFERENCES

Ariathurai, R. and Krone, R. B., 1976, Finite element model for cohesive sediment transport. *Journal of Hydraulic Division ASCE*, (104) 2, 323-328.

Batrakov, G.F., Eremeev, V.N., Chudinovskikh, T.V. and Zemlyanoy, A. D., 1994, Radioactivity of the Black Sea, Ecosi-Hydrophysics, Sevastopol.

BIOMOVS II, 1996, Technical Report No. 10, Assessment of the Consequences of the radioactive Contamination of Aquatic Media and Biota. Model Testing Using Chernobyl Data, Swedish Radiation Protection Institute, Stockholm.

Blumberg, A.F. and Mellor, G.L., 1987. A description of a three dimensional coastal ocean circulation model, In: Three-Dimensional Coastal Ocean Models, N. Heaps (ed), Am. Geoph. Union, Washington, D.C. 1-16.

Carroll, J. and Harms, I.H., 1999, Uncertainty analysis of partition coefficients in a radionuclide transport model, *Water Research*, (33) 11, 2617-2626.

IAEA. Sediment Kd and concentration factors for radionuclides in the marine environment. IAEA Technical Report No.247, International Atomic Energy Agency, Vienna, 1985.

Koziy, L., Maderich, V., Margvelashvili, N. and Zheleznyak, M., 1998, Three-Dimensional model of the radionuclide dispersion in the estuaries and shelf seas. *Journal of Environmental Modeling and Software*, (13) 5-6, 413-421.

Margvelashvili, N., Maderich, V., and Zheleznyak, M., 1997, THREETOX - a computer code to simulate three-dimensional dispersion of radionuclides in stratified water bodies, *Radiation Protection Dosimetry*, (73) 1-4, 177-180.

Margvelashvili, N., Maderich, V.and Zheleznyak, M., 1999, Simulation of radionuclide flux from Dnieper-Bug Estuary into the Black sea, *Journal of Environmental Radioactivity*, (43) 2, 157-171.

Rijn van, L.C., 1984, Sediment transport. Part II: Suspended load transport, *Journal of Hydraulic Engineering*, (110) 11, 1613-1641.

Onishi, Y., Dummuller, D.C. and Trent, D.S., 1989, Preliminary Testing of Turbulence and Radionuclide Transport Modeling in Deep Ocean Environment, Report PNL-6853, Pacific Northwest Laboratory, Richland, Washington.

Perianez, R., 2000, Modelling the tidal dispersion of ^{137}Cs and ^{239,240}Pu in the English Channel, *Journal of Environmental Radioactivity*, (49) 3, 259-277.

Polikarpov, G.G., Timoschuk, V.I. and Kulebakina, L.G., 1988, Concentration of ^{90}Sr in the aquatic environment of Lower Dnieper toward the Black Sea, *Dopovidi (Proceedings) of National Academy of Sciences of Ukraine*, ser. B, 3, 75-76 .

Polikarpov, G.G., Livingston, H.D., Kulebakina, L.G., Buesseler, K.O., Stokozov, N.A. and Casso, S.A., 1992, Inflow of Chernobyl ^{90}Sr to the Black Sea from the Dniepr river, *Journal of Estuarine, Coastal and Shelf Science*, (34) 2, 315-320.

Santschi, P.H., and Honeyman, B.D., 1989, Radionuclides in aquatic environments, *Radiation Physics and Chemistry*, (34) 2, 213-240.

Shiklomanov, I.A. (ed.), 1992, Hydrological, thermal, chemical and radiological regime of the Cooling Pond of Chernobyl NPP, Tech. Report, State Hydrological Institute, Leningrad.

Simonov, A.I. and Altman, E.N. (Eds.), 1991, Hydrometeorology and hydrochemistry of seas of USSR. v.IV, Black sea, 1, Hydrometeorological conditions, Hydrometeorological Publ., S.-Petersburg.

Voitsekhovich, O.V. (ed.), 1997, Radioecology of water objects of the Chernobyl NPP accident impact area, Chernobylinterinform, Kiev.

Zheleznyak, M., 1988. Structure of the bottom turbulent boundary layer under the waves, *Hydromechanics*, (58), 1-8.

Zheleznyak, M. , Demchenko, R., Khursin, S., Kuzmenko, Yu., Tkalich, P. and Vitjuk, N., 1992, Mathematical modeling of radionuclide dispersion in the Pripyat-Dnieper aquatic system after the Chernobyl accident, *The Science of the Total Environment* (112), 1, 89-114.

Zheleznyak, M., Shepeleva, T., Sizonenko, V. and Mezhueva, I., 1997, Simulation of countermeasures to diminish radionuclide fluxes from Chernobyl zone via aquatic pathways, *Radiation Protection Dosimetry*, (73) 1-4, 181-186.